Global Journal of Engineering and Technology Advances
eISSN: 2582-5003
Cross Ref DOI: 10.30574/gjeta
Journal homepage: https://gjeta.com/

(Research Article)

Check for updates

Adaptive particle swarm optimization approach to simultaneous reconfiguration and shunt capacitor allocation in radial distribution network

Ismail Adeyemi ADEYEMO *, Oluwadare Olatunde AKINROGUNDE, Sunday Adeleke SALIMON and Oluwaseyi Wasiu ADEBIYI

Department of Electronic & Electrical Engineering, Ladoke Akintola University of Technology, PMB 4000, Ogbomoso, Oyo State, Nigeria.

Global Journal of Engineering and Technology Advances, 2022, 12(03), 077–094

Publication history: Received on 16 August 2022; revised on 22 September 2022; accepted on 24 September 2022

Article DOI: https://doi.org/10.30574/gjeta.2022.12.3.0162

Abstract

Simultaneous radial distribution network reconfiguration (RDNR) and shunt capacitor allocation (SCA) is one of the compensation techniques that are used for getting an improved radial structure with reduced real power loss and enhanced voltage stability. This study presents a novel adaptive particle swarm optimisation (APSO) technique for the simultaneous RDNR and SCA, which is a complex and nonlinear optimisation problem. Unlike the conventional particle swarm optimization (PSO) technique in which an initial population of particles is randomly generated, the fundamental loop concept is used to populate the search space of APSO with the candidate branches for each tie switch (open branch) in the loop. The candidate branches are preselected with the graph theory. This is done to mitigate infeasible configurations in the optimization process and also to ensure that the conditions for radiality of the network are satisfied. The effectiveness of the proposed APSO technique for simultaneous RDNR and SCA is demonstrated on the standard IEEE 33-bus and Nigerian Ayepe 34-bus RDNs using six event cases. The efficacy of the proposed APSO technique is further validated with the comparison of the observed simulation results with the reported results of similar work implemented with established algorithms like improved binary particle swarm optimization (IBPSO), modified pollinated flower algorithm (MFPA) and mixed integer linear programming (MILP). The result of the comparative study reveals that the proposed APSO technique outperforms the selected algorithms in most of the considered event cases.

Keywords: Adaptive PSO; Radial distribution network; Reconfiguration; Power loss; Shunt capacitor allocation

1. Introduction

The distribution network is the last segment of the electrical power system that connect the end-users of electricity to the grid. Most of the distribution networks are weakly meshed or radial in nature as power flows in a unidirectional manner from the substation to every other parts of the network. Such networks are called radial distribution network (RDN) and they are widely used due to simplicity of operation, cheap cost and easier protection [1]. However, RDNs suffer from high power losses and voltage drop along the feeders of the RDN, which results into voltage magnitude violation at the buses. These problems are attributable to the high resistance to reactance ratio of network as well as proliferation of heavy inductive loads such as transformers, AC induction motors and adjust table speed drive (ASD) in the networks. Studies have shown that 13% of the total generated power is wasted as losses in the distribution network [2]. In addition, about 70% of all the losses in the electrical power system occur in the distribution network. Therefore, efforts are continually made to mitigate bus voltage magnitude violations and power losses, which adversely affect the general performance of the distribution network.

* Corresponding author: Ismail Adeyemi ADEYEMO
Department of Electronic & Electrical Engineering, Ladoke Akintola University of Technology, PMB 4000, Ogbomoso, Oyo State, Nigeria.

In electric power systems, the voltages at all the buses are required to be within acceptable limit. If a power system is operated beyond its voltage stability limit, voltage collapse results. However, with the unabating increase in global power demand and high cost of constructing new power systems, utility providers are constrained to operate very close to the limit resulting in a situation where RDNs are heavily loaded [3]. To improve power system efficiency and forestall voltage collapse, several methods are used to mitigate power losses and improve voltage profile in RDNs. These methods include reconfiguration of the network, load management, and optimal placement of power compensators such as shunt capacitor and distributed generation (DG) [4]. Power compensators are electrical devices that are capable of power injection into power system networks for the enhancement of power transfer capability. They are placed in the distribution networks at the optimal locations in order to mitigate voltage deviation and power losses in the distribution system. However, non-optimal placement and sizing of power compensators may aggravate rather than mitigate power losses. The available methods for the mitigation of RND problems are either implemented singly or combined together in such a way that a better network in terms of power loss reduction, voltage profile improvement. Load balancing, loadability, stability, and reliability is obtained [5]. These methods are usually formulated as a combinatorial optimization problem in which there is a single or multi-objective function subject to certain constraints and limits. From the economic point of view, the cheapest among these methods are the distribution network reconfiguration and shunt capacitor allocation [4].

In this study, radial distribution network reconfiguration (RDNR) and optimal shunt capacitor allocation are simultaneously implemented for power loss reduction and voltage profile enhancement. RDNR involves altering the status of the normally closed branches called sectionalizing switches (SS) and normally open branches called tie switches (TS) of the radial distribution network, which results into an improved radial configuration. Shunt capacitor allocation (SCA) on the other hand, deals with the installation of the appropriate number and size of shunt capacitors at optimal locations in the distribution network. By injecting reactive power into distribution network, shunt capacitor installation does not only provide power loss mitigation, it also improves voltage profile and stability of the network. Allocation of shunt capacitors in distribution network requires proper optimization of placement and sizing. Simultaneous RDNR and SCA combines the strengths of both methods resulting in a vastly improved network in which there is more power loss reduction and a better enhanced voltage profile. Simultaneous implementation of RDNR and SCA is a combinatorial optimization problem that is complex and nonlinear. In recent years, several optimization techniques have been deployed for simultaneous optimization of RDNR and SCA in a bid to maximize the operational efficiency of the RDNs using various indices such as real power loss reduction index, loss sensitivity factor (LSF) and voltage stability index (VSI) as performance evaluation metrics. The real power loss is the total of all the real power losses in all the lines of the RDN under consideration while VSI deals with the acceptable limits of voltage magnitude at each of the distribution network buses as well as load operation stability [3]. RDNs are vulnerable to voltage instability and collapse when operated under stress as a result of overloading. Buses that are close to the point of collapse and in need of compensation are identified using VSI. The bus having the minimum VSI is the most susceptible to voltage collapse.

The optimization techniques that have been presented for power loss mitigation and voltage profile improvement using simultaneous implementation of RDNR and SCA include ant colony search algorithm (ACSA) [6], ant colony optimization (ACO) [8], evolutionary algorithms like genetic algorithm (GA) and its variants [9], [10], [11]. In [12], harmony search algorithm has been utilized for solving the RDNR and SCA combinatorial optimization problem with reduction of power loss and voltage deviation as the objectives. The RDNR and SCA problem was also solved using improved binary particle swarm optimization (IBPSO) in [13]. Juan *et al* proposed mixed-integer second-order cone programming formulation for the optimization problem using voltage dependent models [14]. Other optimization methods like mixed integer linear programming (MILP) [7], ordination optimization [15], bat algorithm [16], oppositional krill herd algorithm (OKHA) [17], cat swarm optimization (CSO) [18], modified flower pollinated algorithm (MFPA) [19], moth swarm algorithm (MSA) [20], chemical reaction optimization (CRO) [21], modified particle swarm optimization (MPSO) [22], and autonomous group particle swarm optimization (AGPSO) [23] have also been deployed to solve RDNR and SCA combinatorial optimization problem. The aforementioned studies in [7] – [23] implemented their solution techniques on standard IEEE radial distribution networks.

The effect of simultaneous implementation of RDNR and SCA on real power loss (RP_{loss}) and voltage stability of radial distribution network is presented in this study. With the power loss minimization as the objective function, simultaneous implementation of RDNR and SCA is formulated as a combinatorial optimization problem, which is then solved using adaptive particle swarm optimization (APSO) technique. The proposed APSO is tested on standard IEEE 33-bus and a practical Nigerian Ayepe 34-bus RDNs. Although the authors in [13], [22] and [23] have worked on the simultaneous implementation of RDNR and SCA using variants of PSO, their techniques suffer from large number of infeasible configurations and radiality constraint violation. This is attributable to the random generation of the initial population of particles in their works. In the proposed APSO, the initial population is generated using graph theory in order to reduce the number of infeasible configurations, and also to prevent radiality constraints violation.

The paper is structured in five sections as follows: Section 1 deals with the introduction. Section 2 entails the objective functions and the constraints of the RDNR and SCA problem. Section 3 discusses the introduction of the particle swarm optimization, its adaptation through graph theory, check of radiality constraints and implementation of the APSO for the RNDR and SCA problem. The results achieved by the proposed APSO are presented and discussed in section 4 while the conclusion of the study is found in section 5.

2. Problem Formulation

2.1. Objective function

The main purpose of reconfiguration of RDN and SCA is total power loss reduction in the network. Hence, this is considered as the objective function of this work. The total power of any RDN is determined by the summation of the losses in the line sections of the system:

$$OF_{min} = RP_{loss} = \sum_{i}^{n_b} |I_i|^2 R_i \text{.........................(1)}$$

Here, OF_{min} is the objective function of real power losses (RP_{loss}), n_b is the total number of branches in the RDN, R_i is the resistance of the ith branch of the RDN and $|I_i|$ is the current magnitude of the ith branch of the RDN.

2.2. Constraints

The optimal size and location of shunt capacitors are found by subjecting the objective function in equation (1) to the following constraints:

- Power flow equations: The power flow equation is solved using the Newton Raphson load flow technique in the optimization process. These equations are given as:

$$P_{gi} = P_{Di} + \sum_{j=1}^{n_b} |V_i| \, |V_j| \left[G_{ij} \cos\theta_{ij} + B_{ij} \sin\theta_{ij} \right] \text{......................... (2)}$$

$$Q_{gi} = Q_{Di} + \sum_{j=1}^{n_b} |V_i| \, |V_j| \left[G_{ij} \sin\theta_{ij} - B_{ij} \cos\theta_{ij} \right] \text{......................... (3)}$$

where V_i and V_j are the voltages of buses 'i' and 'j' respectively; P_{gi} and P_{Di} are the real power generated and power demanded at bus 'i'; Q_{gi} and Q_{Di} are the reactive power generated and demanded at bus 'i'; and θ_{ij} is the difference between the voltage angles of buses 'i' and 'j'.

- Reactive power constraint of SC: The size of the each of the installed shunt capacitors is constrained within the limits:

$$Q_{SC(min)} \leq Q_{SC} \leq Q_{SC(max)} \qquad \text{......................... (4)}$$

Where $Q_{SC(min)}$= 100 kVar and $Q_{SC(max)}$ is 75% of the total reactive power demand of the network [25].

- Bus voltage limitation: The voltage must fall within the standard limits for RDN

$$V_{min} \leq V_i \leq V_{max} \qquad \text{......................... (5)}$$

Where the minimum voltage, V_{min} = 0.95 p.u., the maximum voltage, V_{max} = 1.05 p.u., and V_i is the bus voltage.

- Radial configuration constraint: The radial nature of the RDN must be maintained such that there is just a unidirectional flow of power to all buses associated with the network.

2.3. Performance evaluation metrics

In this study, the efficiency of the proposed APSO for simultaneous RDNR and SCA is evaluated using percentage power loss reduction index (%PLRI) and voltage stability index (VSI).

- Real power loss (RP_{loss}) and percentage power loss reduction index (%PLRI)

Real power loss is the summation of all the real power losses in all the lines of the RDN as given in equation (1). In this study, the percentage power loss reduction index is calculated as given below:

$$\%PLRI = \frac{RP_{loss(before\_RDNR\_SCA)} - RP_{loss(after\_RDNR\_SCA)}}{RP_{loss(before-RDNR\_SCA)}} \times 100\% \quad \text{……………………. (6)}$$

Where $RP_{loss(before\_RDNR\_SCA)}$ and $RP_{loss(after\_RDNR\_SCA)}$ are the power losses of the RDN before and after simultaneous RDNR and DG allocation, respectively.

- Voltage stability index (VSI) and minimum VSI

RDNs are exposed to voltage instability and collapse when operated under stress and overloaded. Voltage stability index is used to identify buses that are close to point of collapse and may need compensation [25]. It is given as follows:

$$VSI = |V_s|^4 - 4[P_r R_{sr} + Q_r X_{sr}]|V_r|^2 - 4[P_r R_{sr} + Q_r X_{sr}] \quad \text{……………………. (7)}$$

Where s and r stand for the sending and receiving end bus. V, P, and Q represent voltage magnitude, real power, and reactive power respectively. R and X represent the resistance and reactance between the sending and receiving bus. The least value of the voltage stability index of RDN is referred to as the minimum VSI (VSI_{min}). The bus having VSI_{min} is the most susceptible to voltage collapse.

3. Particle Swarm Optimization (PSO)

PSO is a swarm intelligence-based stochastic search algorithm proposed by Kennedy and Eberhart [26] in 1995. It was inspired by the social behavior exhibited by a school of fish or a flock of birds. PSO solves optimization problems by deploying a population of candidate solutions called swarm of particles collaborating together in their search of optimal solutions in the search space through successive updating of generations (iterations). Starting with a randomly initialized population of particles moving in random directions, each particle goes through the search space looking for the best position. With each particle having a randomly generated position and velocity, fitness evaluation of all the particles is performed with the objective function. The personal best position of the ith particle of a swarm in an N-dimensional space is called personal best ($Pbest$) and denoted by $P_i = [P_{i1},\ P_{i2}, \dots, P_{iN}]$, while the global best, which is the best position attained by any particle in the swarm is denoted by $P_g = \left[P_{g1},\ P_{g2}, \dots, P_{gN}\right]$. During successive iterations, each particle uses its best previous position ($Pbest$) and that of the whole swarm ($Gbest$) to updates its current velocity and position. Thus, if the ith particle of a swarm in an N-dimensional space is currently having velocity and position vectors given as $V_i^t = [V_{i1},\ V_{i2}, \dots, V_{iN}]$ and $x_i^t = [x_{i1},\ x_{i2}, \dots, x_{iN}]$, respectively during iteration t, the particle then updates its current velocity and position in the next iteration as follows [26]:

$$v_i^{t+1} = (w \times v_i^t) + (C_1 \times rand_1 \times (Pbest_i^t - x_i^t)) + \left(C_2 \times rand_2 \times (Gbest_i^t - x_i^t)\right) \quad \text{……………………. (8)}$$

$$x_i^{t+1} = x_i^t + v_i^{t+1} \quad \text{……………………. (9)}$$

Where w is the inertia weight constant within [0,1], C_1 and C_2 are the cognitive and social coefficients, respectively, $rand_1$ and $rand_2$ are random numbers uniformly distributed between [0, 1]. The combination of parameters w, C_1 and C_2 controls the tradeoff between exploration and exploitation of the search space by the particle. The mechanism used to update the parameters is given in [27]. The process of updating velocity and position in PSO continues until any of the stopping criteria is satisfied.

3.1. Adaptive PSO for RDNR and SCA problem

When the conventional PSO is utilized to solve the problem of RDNR and SCA, the radial constraint imposed on the optimization problem results in a number of infeasible configurations during the initialization and intermediate stages. This occurs because a number of sectionalizing switches (SS) will form the search agents in the population, such that when they are opened (or turned to TS) may result in a non-radial structure or infeasible configuration. Hence, The PSO needs some adaptation to make it efficient for the RDNR problem in other to significantly minimize the number of infeasible configurations. In the proposed adaptive PSO (APSO), the particles (search agents) are generated using the graph theory to minimize the number of infeasible configurations at every stage of the optimization process.

Adaptation of PSO through graph theory for removal of infeasible configuration

In the conventional and variants of PSO, the initial population is randomly generated thereby giving a large number of infeasible configurations in which the radiality constraints is not satisfied. In the proposed APSO, these infeasible configurations are reduced using graph theory. The first step is the formation of an incidence matrix C using the number of branches and buses (line data) of the RDN. The incidence matrix, C has one row for each branch and one column for each bus with an entry c_{ij} in row *i* and column *j* according to the following rules [28]:

$$c_{ij} = \begin{cases} +1\ for\ a\ branch\ i\ directed\ away\ from\ node\ \text{j} \\ -1\ for\ a\ branch\ i\ directed\ \text{toward}\ node\ \text{j} \\ 0\ for\ a\ branch\ i\ \text{not connected to}\ node\ \text{j} \end{cases} \quad \text{……………………. (10)}$$

When all the tie switches (TS) of the RDN are closed, some loops are formed in the network. These loops are referred to as the fundamental loops. The number of fundamental loops (FLs) formed in the RDN is equal to the number of TS [29], [30]. To determine the FLs of the RDN after formation of the incidence matrix, a tie switch (TS) is added to the incidence matrix. Based on the technique utilized in [31], the absolute sum of the corresponding column (S_C) of the matrix after addition of a tie switch is calculated. The branches connected to bus whose S_C is 1 are removed. This process is repeated until branches connected to bus whose S_C are 1 are no longer available in the RDN. The number of branches remaining forms a fundamental loop (FL) and is saved [32]. Thereafter, another TS is added and the whole process is repeated. Figure 1 shows a simple sample of RDN with TSs and the first FL is determined as shown in Figure 2.

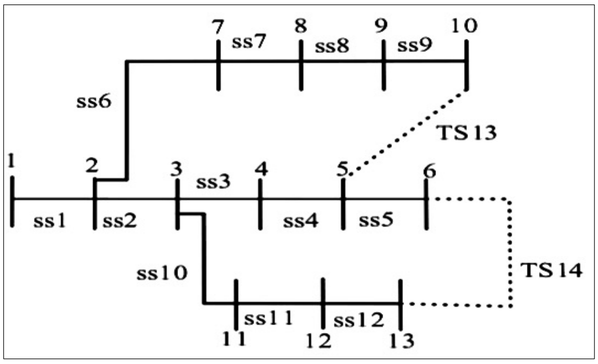

Figure 1 A simple sample of 13-bus RDN

As shown in Figure 2, after determining the incidence matrix, the following steps are executed to identify the FLs.

- Step 1: Add the first tie switch (open branch: TS13) to the incidence matrix C.
- Step 2: Calculate sum of absolute each element of a corresponding column (S_C) in matrix C. The buses which have the S_C as 1, are 1, 6 and 13. The branches 1, 5 and 12 are removed because they are connected to buses 1, 6 and 13, respectively.
- Step 3: Similar to step 2, calculate S_C for the remaining branches in matrix C and the result is that the branch 12 is removed.
- Step 4: Similar to step 2, calculate S_C for the remaining branches in matrix C and the result is that the branch 4 is removed.
- Step 5: There is not any bus whose S_C is 1. Therefore, the first FL consists of branches {2, 3, 4, 6, 7, 8, 9 and 13}. Similar to TS13, by adding TS14, the second FL that consists of branches {3, 4, 5, 10, 11, 12 and 14} will be obtained.

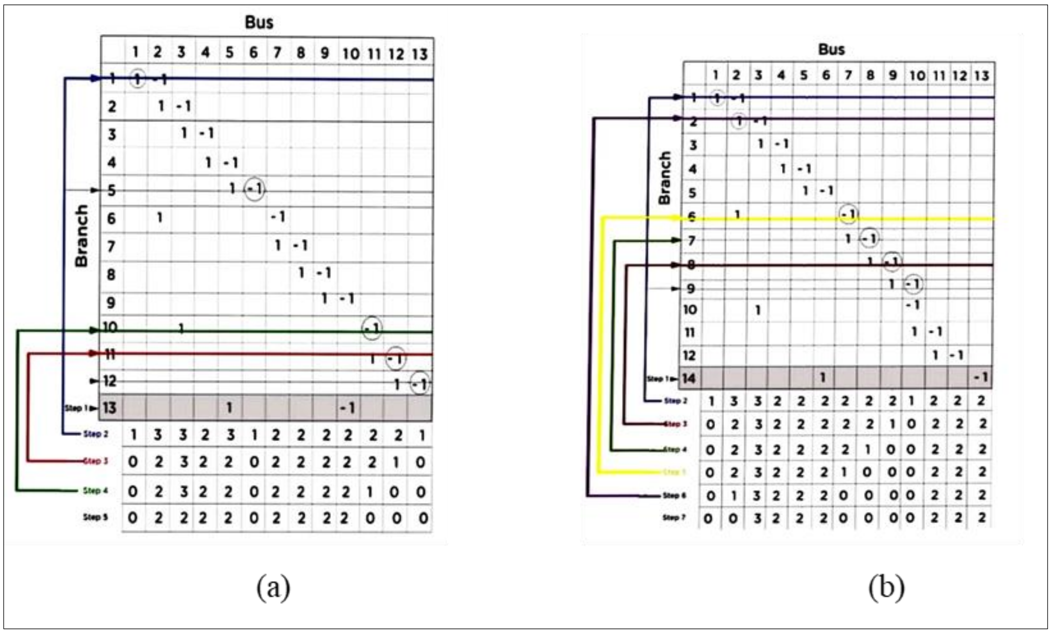

Figure 2 Determination of FLs when closing branches (a) 13 (b) 14

The flowchart for determining the fundamental loops of the RDN is shown in Figure 3. Each radial configuration, which involves a set of open branches are randomly chosen from corresponding FLs. This helps to reduce the generation of infeasible configuration during each stage of the optimization algorithm. However, some of the branches are common in some of FLs [32]. Therefore, radial condition of network must be checked.

3.2. Radial configuration check

In other to satisfy the radial configuration constraints, a radial configuration check is conducted before performing load flow analysis and obtaining the fitness function of each generated solution at various stages of the optimization process of the proposed technique. In each configuration, the incidence matrix C is determined. Then, the first column corresponding to the slack bus in the RDN will be removed to form a square matrix C. If the configuration is radial, the determinant of square matrix C is equal to 1 or -1, otherwise the configuration is non-radial [28]. The flowchart for the radial feasibility of the configuration is shown in Figure 4.

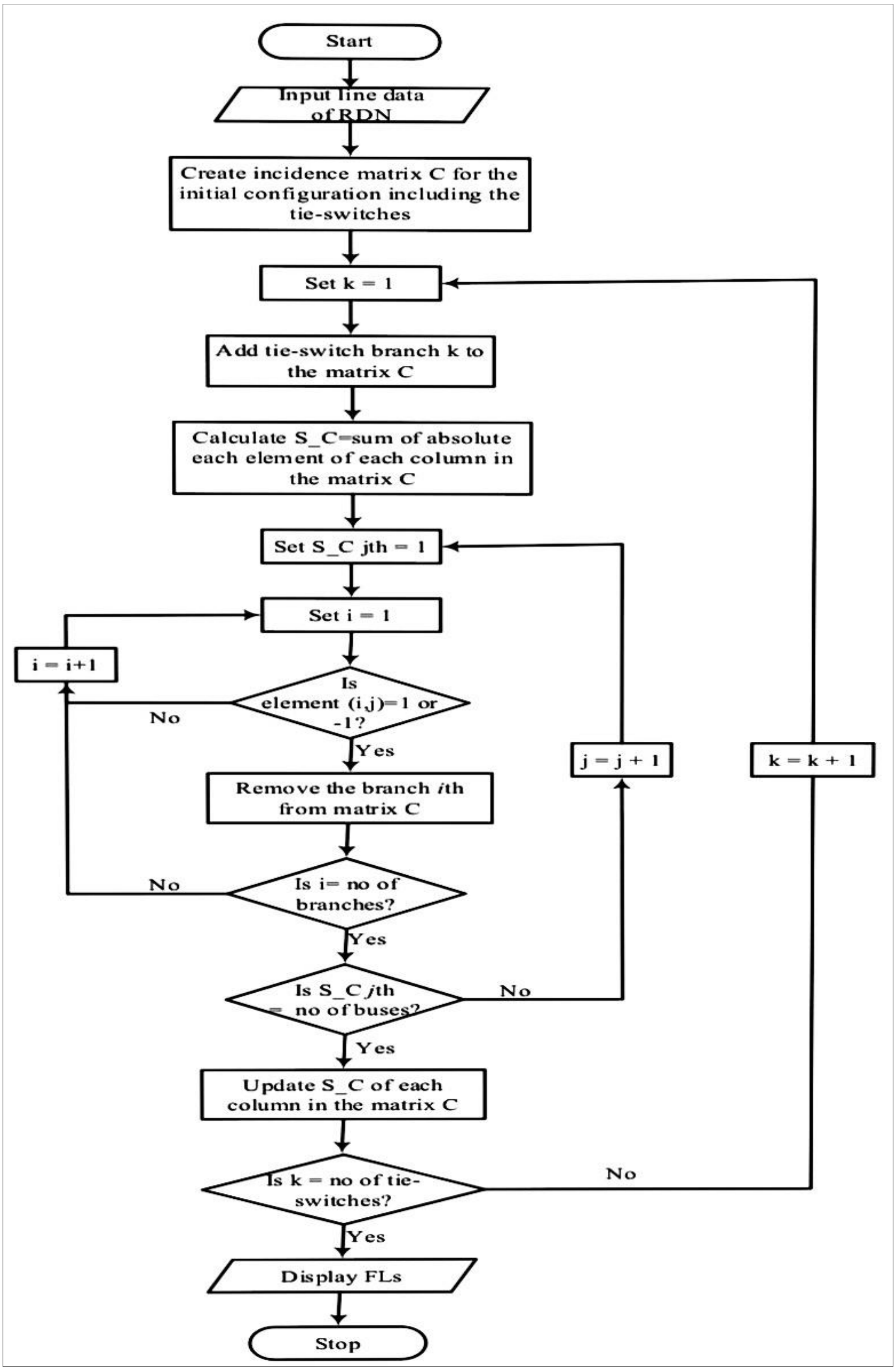

Figure 3 Flowchart for finding fundamental loops (FLs) of any RDN

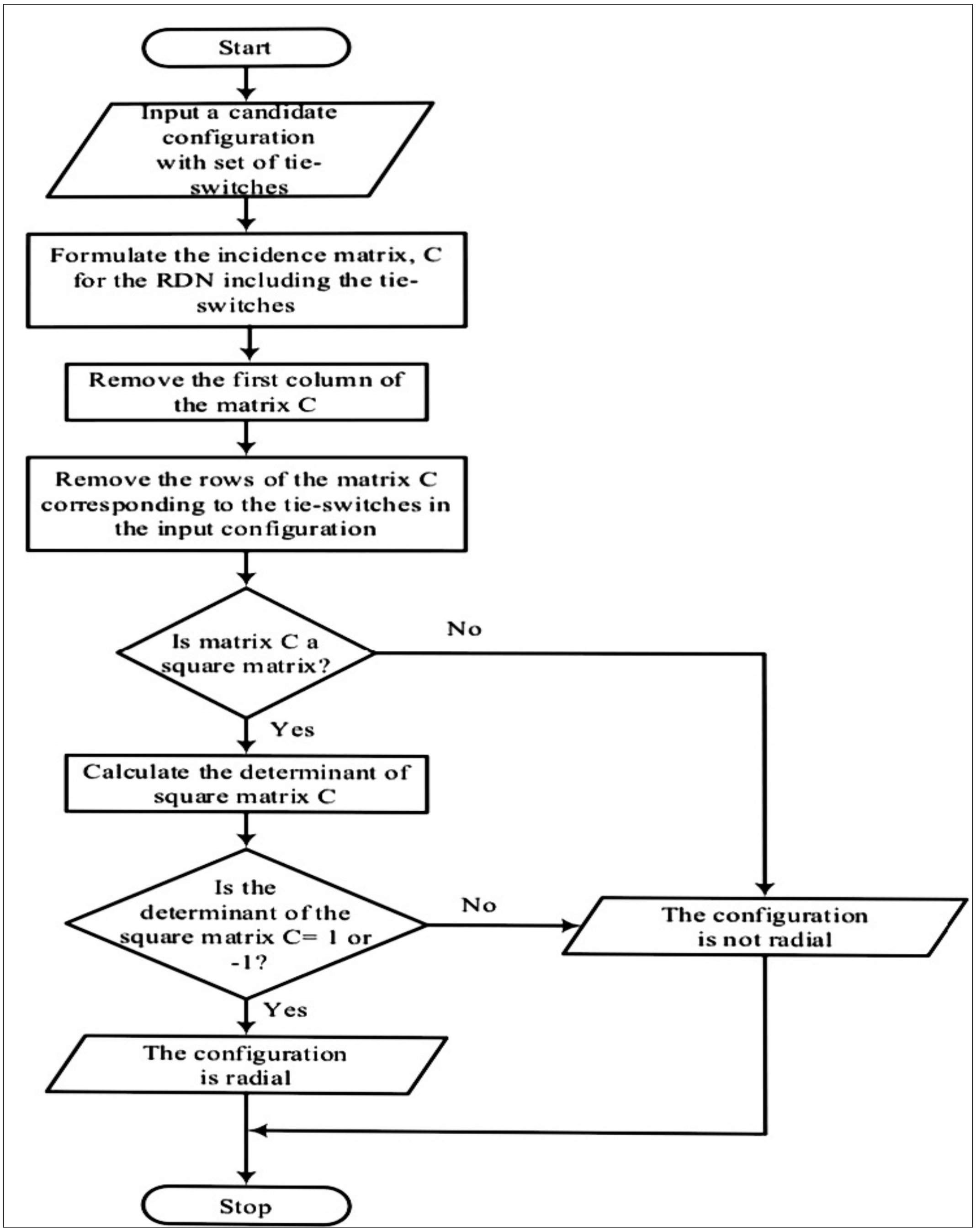

Figure 4 Radiality check for candidate configuration

3.3. Application of APSO for simultaneous RDNR and SCA problem

The steps involved in the implementation of APSO technique for the simultaneous RDNR and SCA are as follows:

- Step 1: Input the line and load data of the RDN including the tie switches, and APSO parameters
- Step 2: Obtain the fundamental loops (FLs) of the RDN using steps given in Figure 3.
- Step 3: Determine the upper-bound and lower-bound of each tie-switch based on the size of the branches that constitute it corresponding FLs.
- Step 4: Initialization

In the application of the APSO technique, a particle is a potential solution consisting of radial configuration, SC locations and SC sizes. A swarm of *n* particles is represented as:

$$X=\begin{bmatrix} x_1 \\ x_2 \\ \vdots \\ x_n \end{bmatrix}=\begin{bmatrix} TS_1^1,\ldots,TS_{NTL}^1 & bus.SC_1^1,\ldots,bus.SC_m^1 & cap.SC_1^1,\ldots,cap.SC_m^1 \\ TS_1^2,\ldots,TS_{NTL}^2 & bus.SC_1^2,\ldots,bus.SC_m^2 & cap.SC_1^2,\ldots,cap.SC_m^2 \\ \vdots\ddots\ddots\ddots\ddots\ddots\vdots & \vdots\ddots\ddots\ddots\ddots\ddots\vdots & \vdots\ddots\ddots\ddots\ddots\ddots\vdots \\ TS_1^n,\ldots,TS_{NTL}^n & bus.SC_1^n,\ldots,bus.SC_m^n & cap.SC_1^n,\ldots,cap.SC_m^n \end{bmatrix} \ldots\ldots\ldots\ldots (11)$$

Each particle in the population can be represented as:

$$x_i=[TS_1^i,\ldots,TS_{NTL}^i \quad bus.SC_1^i,\ldots,bus.SC_m^i \quad cap.SC_1^i,\ldots,cap.SC_m^i]^{`} \ldots\ldots\ldots\ldots (12)$$

It can be seen from equation (12) that the solution vector of each particle contains three parts. The first part represents the number of tie switches or lines (open branches) denoted as $TS_1, TS_2, \ldots, TS_{NTL}$ in the fundamental loops (FL_1 to FL_{NTL}) of the RDN, the second part that is denoted as $bus.SC_1, bus.SC_2, \ldots, bus.SC_m$ represents the buses that are selected for shunt capacitor placement while the third part that is represented as $cap.SC_1, cap.SC_2, \ldots, cap.SC_m$ stands for sizes (or capacities) of the shunt capacitor units in kVar to be installed at the selected buses. Therefore, each particle, x_i of the population is randomly initialized as follows:

$$TS_i=round\left[TS_{lower,r1}^i+rand\times(TS_{upper,r1}^i-TS_{lower,r1}^i)\right] \ldots\ldots\ldots\ldots (13)$$

$$bus.SC_i=round\left[bus_{lower,r2}^i+rand\times(bus_{upper,r2}^i-bus_{lower,r2}^i)\right] \ldots\ldots\ldots\ldots (14)$$

$$cap.SC_i=round\left[cap_{lower,r3}^i+rand\times(cap_{upper,r3}^i-cap_{lower,r3}^i)\right] \ldots\ldots\ldots\ldots (15)$$

where r_1 = 1, 2, . . . NTL, r_2 = 1, 2, . . .m and r_3 = 1, 2 . . . m. $TS_{lower,r1}$ and $TS_{upper,r1}$ are the minimum tie-switch and maximum tie-switch that are encoded in the fundamental loop r_1. Shunt capacitors are placed on any bus of the RDN apart from the slack bus which is the first bus. Hence, the lower limit ($cap_{lower,r2}$) and upper limit ($cap_{upper,r2}$) for the placement of the SC units is from bus 2 to the last bus of the RDN and the capacities of each SC is from 100 kVar to maximum power of SC as given in the inequality constraint of equation (4).

- Step 5: Evaluation of fitness function

Radial configuration check is performed for the swarm of particles. The fitness function of non-radial configuration is set at infinity. The load flow for each of the particle is performed using Newton Raphson technique to determine its fitness value with respect to the objective function, which is taken as the power loss in this study as given in equation (1).

- Step 6: Determine $Pbest$ and $Gbest$

Determine the best position of each particle ($Pbest$) from the previous and current iterations. Choose the particle with best fitness value as $Gbest$ for the swarm during the current iteration.

- Step 7: Update positions and velocities of particles

Update the PSO parameters (w, C_1 and C_2), and calculate the particles velocity and position using equations (8) and (9) subject to the limits specified in equations (13) – (15).

- Step 8: Termination condition

If any of the termination condition is satisfied, output the Gbest, its fitness value and stop the optimization process. Else, increment the number of iteration and go to step 5.

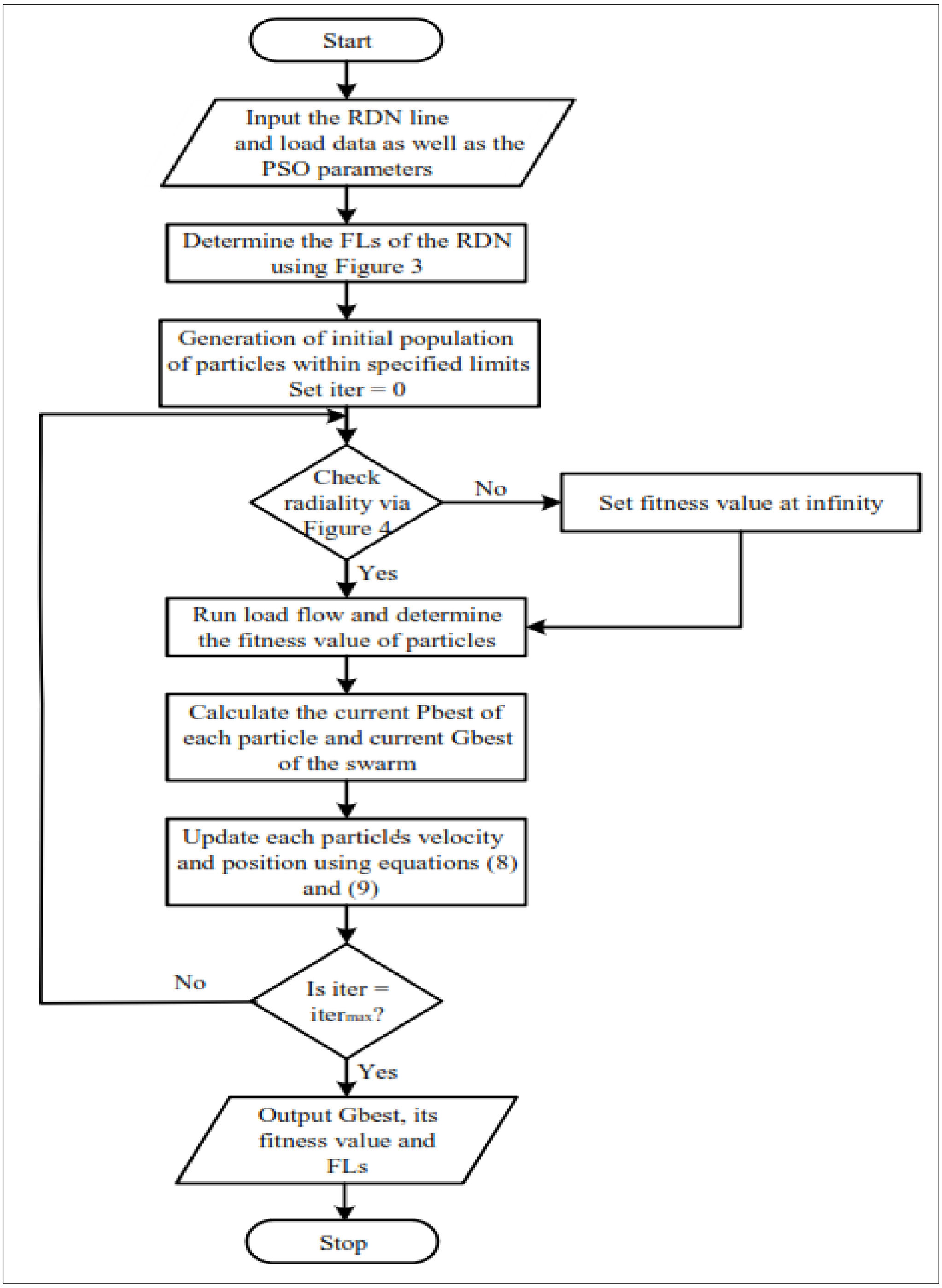

Figure 5 Implementation of the APSO for RDNR and SCA

4. Results and Discussion

The efficacy of the proposed APSO technique in solving the simultaneous RDNR and SCA problem is tested on the IEEE 33-bus and Nigerian Ayepe 34-bus of the Ibadan Electricity Distribution Company (IBEDC) using the MATLAB simulation software (R2021a) on a core i3 laptop clocked at 1.70 GHz. The line and load data of the two test RDNs are found in [33] and [34]. The 33-bus RDN consist of 37 branches made up of 32 sectionalizing switches (SS), 5 tie switches (TS) while the Ayepe 34-bus RDN consists of 38 branches made up of 33 sectionalizing switches (SS) and 5 tie switches (TS). The total number of shunt capacitors available for placement in the RDN is limited to three in this study. The parameters of the APSO utilized in the study are swarm size, n = 1000, and maximum number of iterations, $iter_{max}$ is 200. To demonstrate the global exploration and local exploitation capabilities of the proposed APSO, six different scenarios that are considered are as follows:

- Scenario 1: Base case (BC) without RDNR and SCA
- Scenario 2: Reconfiguration (RDNR) only
- Scenario 3: SCA only
- Scenario 4: SCA after RDNR
- Scenario 5: RDNR after SCA
- Scenario 6: Simultaneous RDNR and SCA

4.1. IEEE 33-bus RDN

The fundamental loops obtained for the 33-bus RDN are depicted in Table 1. The tie-switches displayed in the table gives the boundary and limits of the possible open branches for each of the FLs.

Table 1 Fundamental loops (FLs) of the IEEE 33-bus RDN

loop (FLs)	Tie-switch (TS)
FL1	2, 3, 4, 5, 6, 7, 18, 19, 20, 33
FL2	9, 10, 11, 12, 13, 14, 34
FL3	2, 3,4, 5, 6, 7, 8, 9, 10, 11, 18, 19, 20, 21, 35
FL4	6, 7, 8, 9, 10, 11, 12, 13, 14, 15, 16, 17, 25, 26, 27, 28, 29, 30, 31, 32, 36
FL5	3, 4, 5, 22, 23, 24, 25, 26, 27, 28, 37

The results obtained for all the considered scenarios are given in Table 2. As shown in the table, the power loss (in kW) for the base case (BC) scenario is 202.70. The initial power loss is significantly reduced to 139.997, 132.19, 95.14, 93.49 and 92.64 for scenarios 2, 3, 4, 5 and 6, respectively; corresponding to percentage power loss reduction (%PLR) of 30.94, 34.79, 53.06, 53.88 and 54.30. It is clearly seen from the Table that the minimum voltage has significantly improved for all the considered scenarios compared to the BC. The minimum voltage (bus location) increased from 0.9131 (18) to 0.9413 (32), 0.9377 (18), 0.9561 (33), 0.9597 (33) and 0.9561 (33) for scenarios 2 to 6, respectively. Similarly, the minimum VSI improved from 0.6956 observed in the base case to 0.7850, 0.7733, 0.8366, 0.8482 and 0.8354 for scenarios 2 to 6, respectively. A comparison of all the scenarios reveals that scenario 6 gave the highest percentage power loss reduction demonstrating the superiority of simultaneous RDNR and SCA to the other scenarios.

Table 2 Summary and comparison of results for the various scenarios for the 33-bus RDN

Scenario	Parameters	Proposed APSO	IBPSO [14]	MFPA [20]	MLIP [7]
Scenario 1 (Base Case)	TS	---------	---------	---------	---------
	RP_{loss} (kW)	202.70	202.67	202.67	202.67
	V_{min} (p.u.)	0.9131	0.9131	0.9131	0.9131
	VSI_{min} (p.u.)	0.6956	---------	---------	---------
Scenario 2 (RDNR only)	TS	7 9 14 28 32	7 9 14 32 37	7 9 14 32 37	7 9 14 32 37
	RP_{loss} (kW)	139.997	139.55	139.54	139.54
	% PLRI	30.94	31.14	31.14	31.14
	V_{min} (p.u.)	0.9413 (32)	0.9378	0.9378	0.9378
	VSI_{min} (p.u.)	0.7850	---------	---------	---------
Scenario 3	TS	33 34 35 36 37	33 34 35 36 37	33 34 35 36 37	33 34 35 36 37

(SCA only)	SC size in kW (location)	379 (13) 544 (24) 1037 (30)	900(1) 300(3) 300(14) 300(22) 300(24) 600(30) 600(31)	350 (13) 550 (24) 1050 (30)	750 (6) 150 (28) 850 (29)
	RP_{loss} (kW)	132.19	134.20	132.20	139.57
	% PLRI	34.79	33.78	34.77	31.13
	V_{min} (p.u.)	0.9377 (18)	0.9389	0.9369	0.9302
	VSI_{min} (p.u.)	0.7733	---------	---------	---------
Scenario 4 (SCA after RDNR)	TS	7 9 14 28 32	7 9 14 32 37		
	SC size in kW (location)	626 (21) 489 (24) 922 (30)	1200(4) 900(7) 1800(8) 1200(9) 300(16) 600(30) 600(31)		
	RP_{loss} (kW)	95.14	94.26		
	% PLRI	53.06	53.48		
	V_{min} (p.u.)	0.9561 (33)	0.9612		
	VSI_{min} (p.u.)	0.8366	---------		
Scenario 5 (RDNR after SCA)	TS	7 9 14 36 37	7 10 34 36 37		
	SC size in kW (location)	379 (15) 544 (24) 1037 (30)	900(1) 300 (3) 300(14) 300(22) 300(24)		
	RP_{loss} (kW)	93.49	95.91		
	% PLRI	53.88	52.67		
	V_{min} (p.u.)	0.9597 (33)	0.9658		
	VSI_{min} (p.u.)	0.8482	---------		
Scenario 6 (RDNR and SCA)	TS	7 9 14 32 34	7 9 14 32 37		7 9 14 36 37
	SC size in kW (location)	516 (24) 624 (21) 961 (30)	600(7) 300(12) 300(25) 600(30) 300 (33)		200 (28) 200 (29) 550(30)
	RP_{loss} (kW)	92.64	93.06		101.77
	% PLRI	54.30	54.07		49.78
	V_{min} (p.u.)	0.9561 (33)	0.9585		0.9585
	VSI_{min} (p.u.)	0.8354	---------		---------

The voltage profiles and VSIs for all the considered scenarios are displayed in Figures 6 and 7, respectively. As clearly shown in the figures, bus voltages and VSIs are significantly improved for scenarios 2 to 6.

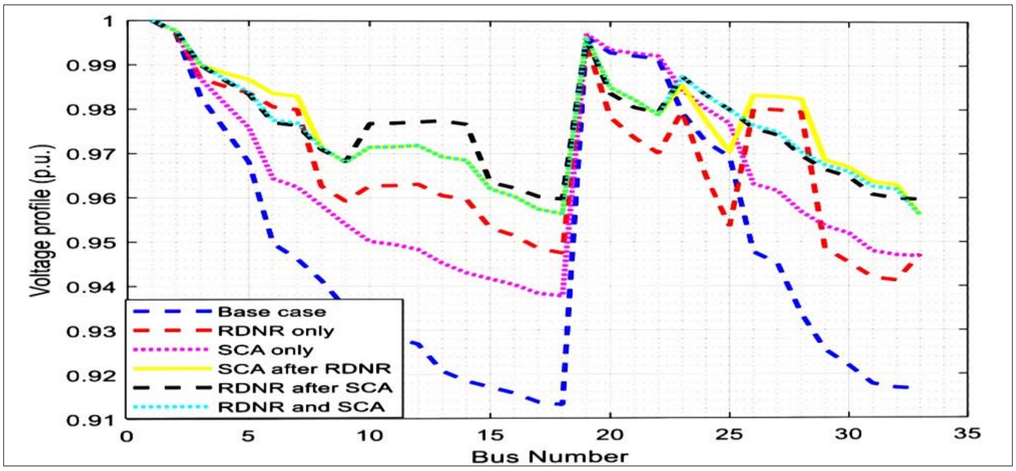

Figure 6 Voltage profile of scenarios 1 – 6 for IEEE 33-bus RDN

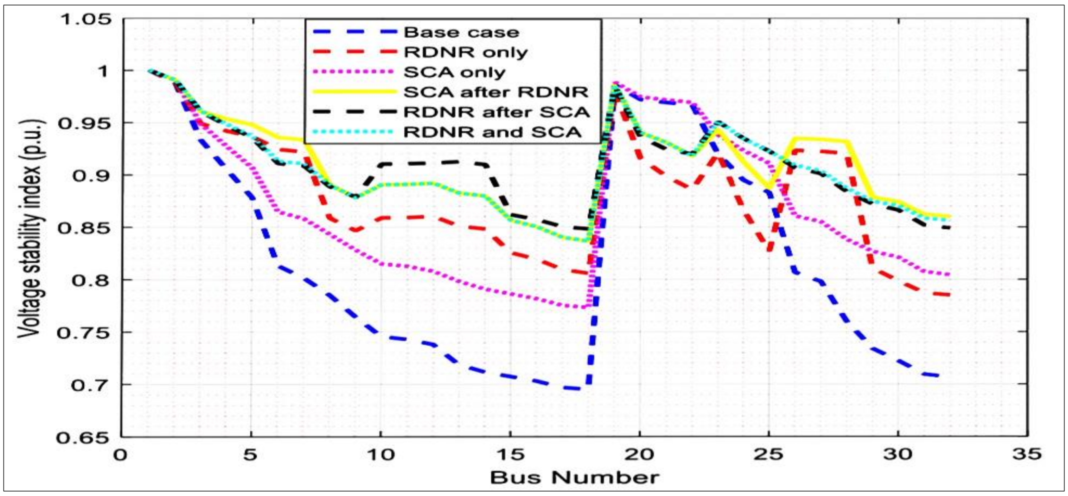

Figure 7 Voltage stability index for scenarios 1 – 6 for IEEE 33-bus RDN

The convergence characteristics of scenarios 2 to 6 are illustrated in Figure 8. It can be seen that scenario 6 (simultaneous RDNR and SCA) has the least power loss closely followed by scenarios 4 and 5.

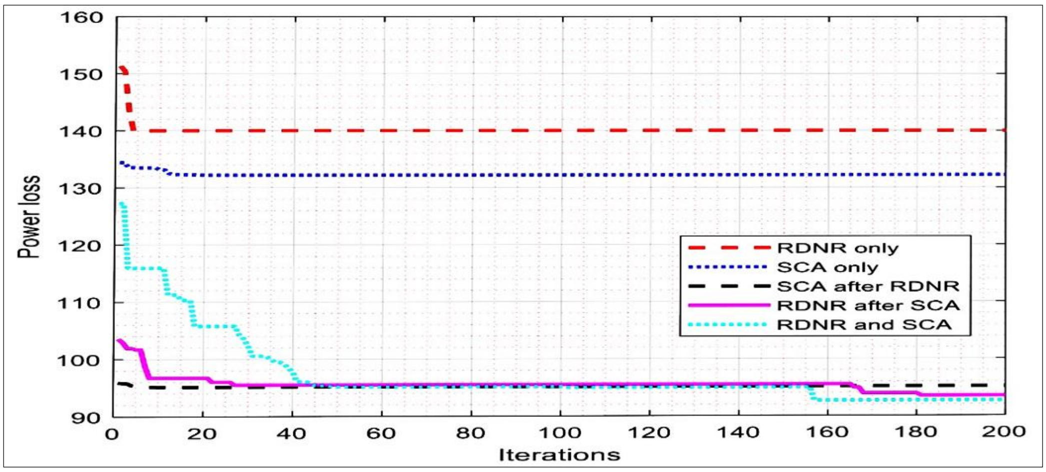

Figure 8 Convergence characteristics of scenarios 2 – 6 for IEEE 33-bus RDN

For further validation of the proposed APSO technique, the observed simulation results in this study are objectively compared with the results of improved binary particle swarm optimization (IBPSO) [14], modified flower pollinated algorithm (MFPA) [20] and mixed integer linear programming (MILP) [7], which are some of the recent literatures that considered the same scenarios. The results of the comparative analysis presented in Table 2 show that the proposed APSO method outperforms the IBPSO, MFPA and MILP in most of the considered scenarios in terms of percentage power loss reduction.

4.2. Nigerian Ayepe 34-bus RDN

The fundamental loops obtained for the Ayepe 34-bus RDN are depicted in Table 3. The tie-switches displayed in the Table gives the boundary and limits of the possible open branches for each of the FLs.

Table 3 Fundamental loops (FLs) of Ayepe 34-bus RDN

Fundamental loops (FLs)	**Tie-switch (TS)**
FL_1	8, 9, 10, 11, 12, 13, 19, 20, 34
FL_2	9, 15, 16, 35
FL_3	12, 13, 19, 20, 21, 36
FL_4	17, 12, 13, 14, 30, 31, 32, 37
FL_5	24, 23, 22, 21, 20, 19, 25, 26, 27, 28, 38

Presented in Table 4 are the results obtained for all the considered cases. As displayed in the table, the power loss (in kW) for the BC scenario is 762.00. The initial power loss (in kW) is significantly reduced from 762.00 to 622.43, 587.17, 483.1, 481.97 and 478.64 for scenarios 2, 3, 4, 5 and 6, respectively; with a corresponding percentage power loss reduction (%PLR) of 18.32, 22.94, 36.60, 36.75 and 37.19, respectively. It is clearly seen from Table 4 that the minimum voltage significantly improved for scenarios 2 to 6 compared to scenario 1, which is the base case. The minimum voltage and corresponding (bus location) increased from 0.8332 (24) observed in the base case to 0.8599 (25), 0.8491 (25), 0.8757 (35), 0.8781 (27) and 0.8773 (34) for scenarios 2 to 6, respectively. Similarly, there is an improvement in minimum VSI from 0.4743 (25) to 0.5192 (24), 0.5195 (23), 0.5715 (29), 0.5839 (25) and 0.5807 (24) for scenarios 2 to 6, respectively. A comparison of all the scenarios reveals that scenario 6 gave the highest percentage power loss reduction demonstrating the efficiency of simultaneous RDNR and SCA.

Table 4 Summary of results for the various scenarios for the Ayepe 34-bus RDN

Items	**Base Case**	**RDNR**	**SCA**	**SCA after RDNR**	**RDNR after SCA**	**RDNR and SCA**
TS	34 35 36 37 38	15 13 23 31 21	34 35 36 37 38	13 15 21 23 31	12 14 15 21 23	12 14 15 21 23
SC size (kVar)			531 (9) 1032(14) 344 (23)	433 (7) 783 (12) 736 (26)	531 (9) 1032 (14) 344 (23)	833 (12) 640 (21) 358 (28)
RP_{loss} (kW)	762	622.43	587.17	483.1	481.97	478.64
%PLRI	-------------	18.32	22.94	36.60	36.75	37.19
V_{min} (p.u.)	0.8332 (24)	0.8599 (25)	0.8491 (25)	0.8757 (35)	0.8781 (27)	0.8773 (34)
VSI_{min} (p.u.)	0.4743 (25)	0.5192 (24)	0.5195 (23)	0.5715 (29)	0.5839 (25)	0.5807 (24)

The voltage profiles and VSIs for all the considered scenarios are displayed in Figures 9 and 10. It is clear from the figures that the bus voltages and VSIs significantly improve in scenario 2 to 6.

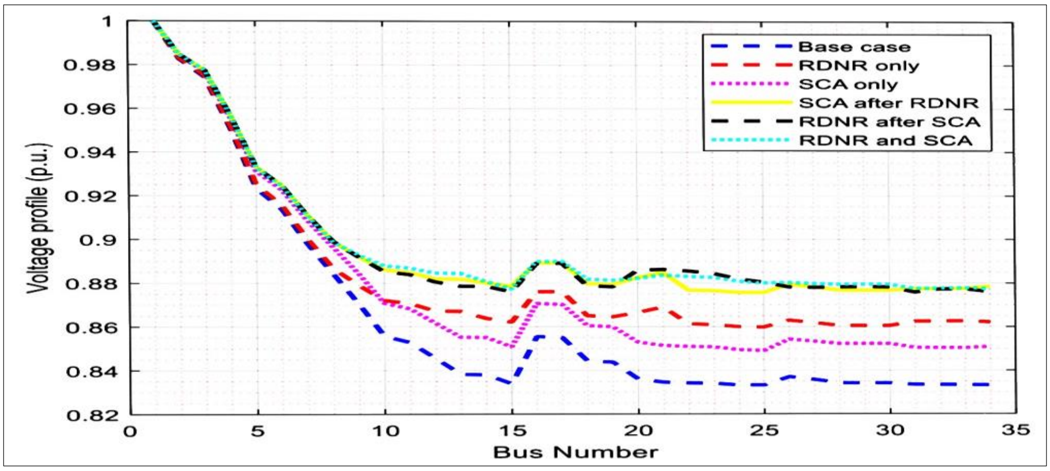

Figure 9 Voltage profile of scenarios 1 – 6 for Ayepe 34-bus RDN

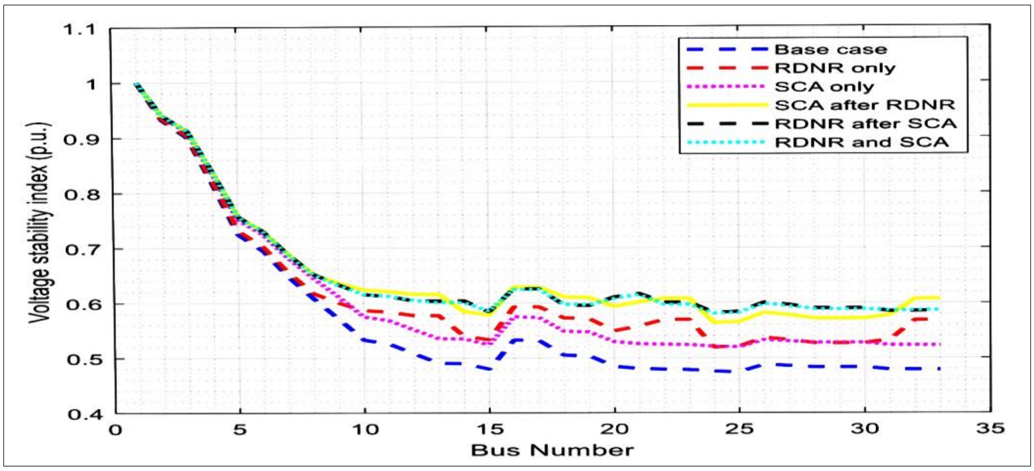

Figure 10 Voltage profile of scenarios 1 – 6 for Ayepe 34-bus RDN

The convergence characteristics of scenarios 2 to 6 are illustrated in Figure 11. It can be seen that scenario 6 (simultaneous RDNR and SCA) has the least power loss closely followed by scenarios 4 and 5.

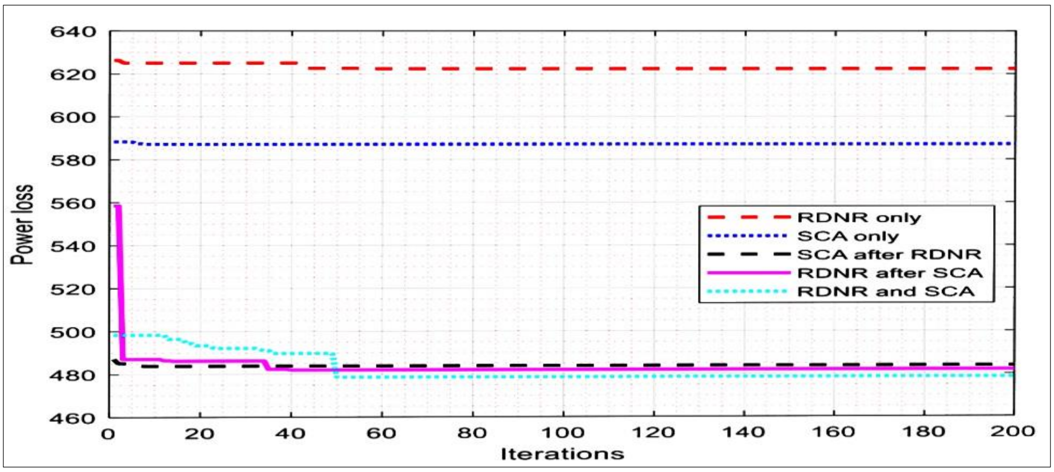

Figure 11 Convergence characteristics of scenarios 2 – 6 for Ayepe 34-bus RDN

5. Conclusion

In this paper, an adaptive particle swarm optimization (APSO) is proposed for solving the combinatorial optimization problem that characterize simultaneous implementation of radial distribution network reconfiguration (RDNR) and shunt capacitor allocation (SCA) with the aim of reducing the power loss in practical radial distribution networks. In the proposed APSO method, the graph theory is used for the adaptation of the tie switches search space in an effort to significantly minimize the infeasible configurations in the optimization process and perform the radiality constraints check of the generated configurations. In a bid to establish the effectiveness of the proposed method, six different scenarios, which are the base case without RDNR and SCA, RDNR only, SCA only, SCA after RDNR, RDNR after SCA and simultaneous RDNR and SCA are considered. The proposed APSO is tested on standard IEEE 33 RDN and Nigerian Ayepe 34-bus RDN. The simulation results reveal that simultaneous RDNR and SCA outperforms the other considered scenarios in term of power loss reduction and voltage profile improvement. Further validation of the efficacy of the proposed technique was also performed by comparing the observed simulation results of the IEEE 33-bus with the reported results of IBPSO, MFPA and MILP algorithms for similar scenarios that are available in open literatures. The result of the comparative study reveals that the proposed APSO technique outperforms the selected algorithms in most of the considered event cases.

Compliance with ethical standards

Acknowledgments

The authors appreciate the staff and management of Ibadan Electricity Distribution Company (IBEDC) for the provision of the line and load data of Nigerian Ayepe 34-bus distribution network.

Disclosure of conflict of interest

The authors declare that they do not have any conflict of interest.

References

[1] Sallam AA, Malik OP. Electric Distribution System Modeling. Piscataway, NJ: IEEE press; 2011.

[2] Rao RS, Narasimham SVL, Ramalingaraju M. Optimal Capacitor Placement in a Radial Distribution System using Plant Growth Simulation Algorithm. International Journal of Electrical Power & Energy Systems. 2011; 33(5), 1133-1139.

[3] Murthy GVK, Sivanagaraju S, Satyanarayana S, Rao BH. Voltage Stability Index of Radial Distribution Network with Distributed Generation. International Journal of Electrical Engineering. 2012; 5(6): 791-803.

[4] Kumar N, Ramraj M. Combined Reconfiguration and Capacitor Placement for Distribution System Volt/Var Control through Opposition Based Differential Evolution Algorithm. Automatika. 2015; 56(2): 140-148. https://doi.org/10.7305/automatika.2015.07.611

[5] De Macedo Braz HD, De Souza BA. Distribution Network Reconfiguration using Genetic Algorithms with Sequential Encoding: Subtractive and Additive Approaches. IEEE Transaction Power System. 2011; 26(2): 582 – 93.

[6] Chang CF. Reconfiguration and Capacitor Placement for Loss Reduction of Distribution Systems by Ant Colony Search Algorithm. IEEE Transaction Power System. 2008; 23(4): 1747 – 1755.

[7] Gallego LA, López-Lezama JM, Carmona OG. A Mixed-Integer Linear Programming Model for Simultaneous Optimal Reconfiguration and Optimal Placement of Capacitor Banks in Distribution Networks. IEEE Access. 2022; 10: 52655-52673.

[8] Divya BRM. Simultaneous Network Reconfiguration and Capacitor Placement for Loss Reduction of Distribution Systems by Ant Colony Optimization Algorithm. Int. J. Adv. Electr. Electron. Eng. 2012; 1(2): 211 - 220.

[9] Díaz RH, Harnisch VI, Sanhueza HR, Olivares RR. Feeder Reconfiguration and Capacitor Placement in Distribution Systems: An Approach for Simultaneous Solution using a Genetic Algorithm. Ingeniare. Revista Chilena de Ingeniería. 2010; 18(1): 144 - 153.

[10] Guimarães MAN, Castro CA. An Efficient Method for Distribution Systems Reconfiguration and Capacitor Placement using a Chu-Beasley Based Genetic Algorithm. In Proc. IEEE Trondheim Power Tech. 2011: 1-7.

[11] Farahani V, Vahidi B, Abyaneh HA. Reconfiguration and Capacitor Placement Simultaneously for Energy Loss Reduction Based on an Improved Reconfiguration Method. IEEE Trans. Power System. 2012; 27(2): 587 - 595.

[12] Rao RS. An Hybrid Approach for Loss Reduction in Distribution Systems using Harmony Search Algorithm. Int. J. Electr., Comput., Energetic, Electron.Commun. Eng., 2010; 4(3): 557 - 563.

[13] Sedighizadeh M, Dakhem M, Sarvi M, Kordkheili H. Optimal Reconfiguration and Capacitor Placement for Power Loss Reduction of Distribution System using Improved Binary Particle Swarm Optimization. Int. J. Energy Environ. Eng. 2014; 5(1): 3.

[14] Juan M. Home-Ortiz JM, Vargas R, Macedo LH, Romero R. Joint Reconfiguration of Feeders and Allocation of Capacitor Banks in Radial Distribution Systems considering Voltage-Dependent Models. Electrical Power and Energy Systems. 2019; 107: 298–310.

[15] Ramli RE, Awad M, Jabr RA. Ordinal Optimization for Optimal Capacitor Placement and Network Reconfiguration in Radial Distribution Networks. In Proc. IEEE Int. Conf. Syst., Man, Cybernetics (SMC). 2012; 1712-1717.

[16] Askari MR. A New Optimization Framework to Solve the Optimal Feeder Reconfiguration and Capacitor Placement Problems,'' Int. J. Sci. Technol. Res. 2015; 4: 23-29.

[17] Sultana S, Roy PK. Oppositional Krill Herd Algorithm for Optimal Location of Capacitor with Reconfiguration in Radial Distribution System. Int. J. Electr. Power Energy Syst. 2016; 74: 78 - 90.

[18] Hosseinnia MFH. Effect of Reconfiguration and Capacitor Placement on Power Loss Reduction and Voltage Profile Improvement,'' Trans. Electr. Electron. Mater. 2017; 18(6): 345-349.

[19] Namachivayam G, Chandramohan S, Perumal SK, Devanathan ST. Reconfiguration and Capacitor Placement of Radial Distribution Systems by Modified Flower Pollination Algorithm. Electric Power Components and Systems. 2016; 44(13): 1-11.

[20] Mohamed E, Al-Attar M, Mitani Y. MSA for Optimal Reconfiguration and Capacitor Allocation in Radial-Ring Distribution Networks. International Journal of Interactive Multimedia and Artificial Intelligence. 2018; 5(1): 107-122.

[21] Roy PK, Sultana S. Optimal Reconfiguration of Capacitor-Based Radial Distribution System using Chaotic Quasi Oppositional Chemical Reaction Optimization. Microsystem Technologies. 2022; 28(2): 499-511.

[22] Gebru Y, Bitew D, Aberie H, Gizaw K. Performance Enhancement of Radial Distribution System using Simultaneous Network Reconfiguration and Switched Capacitor Bank Placement. Cogent Engineering. 2021; 8(1).

[23] G. Srinivasan. Optimization of Distributed Generation Units in Reactive Power Compensated Reconfigured Distribution Network. Automatika. 2021; 62(2): 249-263.

[24] Ali ES, Abd Elazim SM, Abdelaziz AY. Improved Harmony Algorithm and Power Loss Index for Optimal Locations and Sizing of Capacitors in Radial Distribution Systems. Int. J. Electr. Power Energy Syst. 2016; 80, 252–263.

[25] Tan WS, Hassan MY, Majid MS, Rahman, HA. Allocation and Sizing of DG using Cuckoo Search Algorithm. 2012 IEEE International Conference on Power and Energy (PECon). 2012; 133-138.

[26] Eberhart RC, Kennedy J. A new optimizer using Particles Swarm Theory. Sixth International Symposium on Micro Machine and Human Science; Nagoya, Japan; 1995; 39–43.

[27] Mirjalili S, Lewis A, Sadiq AS. Autonomous Particles Groups for Particle Swarm Optimization. Arabian Journal for Science and Engineering. 2014; 39(6): 4683–4697.

[28] Mohammadi M, Rozbahani AM, Bahmanyar S. Power Loss Reduction of Distribution Systems using BFO-Based Optimal Reconfiguration along with DG and Shunt Capacitor Placement Simultaneously in Fuzzy Framework. Journal of Central South University. 2017; 24(1): 90-103.

[29] Gupta N, Swarnkar A, Niazi KR, Bansal RC. Multi-Objective Reconfiguration of Distribution Systems using Adaptive Genetic Algorithm in Fuzzy Framework. IET generation, transmission & distribution. 2010; 4(12): 1288-98.

[30] Dolatdar E, Soleymani S, Mozafari B. A New Distribution Network Reconfiguration Approach using a Tree Model. International Journal of Computer and Information Engineering. 2009; 3(10): 2480-2487.

[31] Nguyen TT, Truong AV, Phung TA. A Novel Method Based on Adaptive Cuckoo Search for Optimal Network Reconfiguration and Distributed Generation Allocation in Distribution Network. International Journal of Electrical Power & Energy Systems, 2016; 78, 801-815.

[32] Dolatdar E, Soleymani S, Mozafari B. A New Distribution Network Reconfiguration Approach using a Tree Model. International Journal of Computer and Information Engineering. 2009; 3(10): 2480-2487.

[33] Baran ME, Wu FF. Network Reconfiguration in Distribution Systems for Loss Reduction and Load Balancing. IEEE Transaction on Power Delivery. 1989; 4(2): 1401-1414.

[34] Adepoju GA, Salimon SA, Aderinko HA, Bisiriyu AO. Optimal Placement and Sizing of Distributed Generation in a Nigerian Distribution Network using Cuckoo Search Algorithm. Current Journal of Applied Science and Technology. 2019; 38(6): 1-12.